Research Article

Hend A. Gad, Ahmed A. Tayel*, Mohammed S. Al-Saggaf, Shaaban H. Moussa, and Amany M. Diab

Phyto-fabrication of selenium nanorods using extract of pomegranate rind wastes and their potentialities for inhibiting fish-borne pathogens

https://doi.org/10.1515/gps-2021-0049
received May 25, 2021; accepted July 14, 2021

Abstract: The invasion of fish/seafoods by zoonotic pathogens causes health threats to humans. Plant derivatives and phytosynthesized nanometals could promisingly overcome bacterial infections/contaminations. The extract of pomegranate rinds (PRE) was innovatively employed for biosynthesizing selenium nanorods (Se-NRs). These agents were assessed as antibacterial candidates against diverse fish-borne pathogenic species (*Staphylococcus aureus*, *Pseudomonas aeruginosa*, *Escherichia coli*, *Salmonella typhimurium*, and *Sphingomonas paucimobilis*). The PRE-synthesized Se-NRs, within 60 min of contact, were negatively charged (−32 mV) and had mean diameter of 62.31 nm and length range of 443.5–1236.9 nm. The designated infrared spectra for PRE and PRE/Se-NRs composite validated the biosynthesis, bonding, and interactions of the nanocomposite. The antibacterial potentialities of PRE, phytosynthesized Se-NRs, and PRE/Se-NRs composite was confirmed toward the entire challenged pathogens; *S. aureus* had the highest resistance (with inhibitory concentrations of 72.5, 60.0, and 55.0 mg/L, respectively) and *S. paucimobilis* was the most sensitive (with inhibitory concentrations of 55.0, 45.0, and 42.5 mg/L, respectively). The ultrastructure of the treated *S. paucimobilis* with PRE/Se-NRs emphasized the composite potentiality for deforming/distorting cells within 4 h and causing full cells' destruction and deformation within 8 h of exposure. The PRE-phytosynthesized Se-NRs are advocated as potent antibacterial products against fish-borne pathogens for decontaminating fisheries farms and products.

Keywords: antimicrobial action, bacterial pathogens, green synthesis, nanocomposite

1 Introduction

Nanotechnology is the fast-growing discipline of science and technology, which targets the production, characterization, and applications of novel materials in nanoforms, e.g., with particles' diameter in nanometer scale [1]. The nanoparticles' (NPs') applications and features effectually served in numerous fields, including chemical, mechanical, optical, and biomedical applications [2]. NPs represent entirely new and augmented features than bulk particles based on their particular properties, e.g., greater surface area, diminished size, distribution, and morphology. Ordinarily, NPs were synthesized via chemical/physical approaches; the physical methods' disadvantages include their high requirements of energy and cost and the low NPs yield, whereas chemical methods frequently cause ecological and toxicological consequences because of the involvement of hazardous chemicals in synthesis and their residues' effects [3,4].

The bio (green) synthesis of NPs could overcome most of the above disadvantages by providing facile, eco-friendly, and economical approaches that apply microorganisms, algae, biopolymers, plant materials, or their derivatives for NPs synthesis [2,5].

* **Corresponding author: Ahmed A. Tayel,** Faculty of Aquatic and Fisheries Sciences, Department of Fish Processing and Biotechnology, Kafrelsheikh University, Kafr El Sheikh, Egypt, e-mail: tayel_ahmad@yahoo.com, ahmed_tayel@fsh.kfs.edu.eg, tel: +20-1001969909
Hend A. Gad: Faculty of Aquatic and Fisheries Sciences, Department of Fish Processing and Biotechnology, Kafrelsheikh University, Kafr El Sheikh, Egypt
Mohammed S. Al-Saggaf: Department of Biology, College of Science and Humanitarian Studies, Shaqra University, Shaqra, Saudi Arabia
Shaaban H. Moussa: Department of Biology, College of Science and Humanitarian Studies, Shaqra University, Shaqra, Saudi Arabia; Department of Microbial Biotechnology, Genetic Engineering and Biotechnology Research Institute, University of Sadat City, Sadat City, Egypt
Amany M. Diab: Faculty of Aquatic and Fisheries Sciences, Department of Aquaculture, Kafrelsheikh University, Kafr El Sheikh, Egypt

Selenium (Se), the essential element for higher organisms' life, is required at 40–300 µg in daily intakes for human. Se at these concentrations is necessary for conventional maintenance of organisms' functions, but it may cause toxicity at high dosage intakes (≥3,200 µg/day) [6,7]. However, the Se nanostructures (e.g., spheres, nanorods, nanowires, hexagonal prism, amorphous, nanotubes, nanoribbons, trigonal, and nanoplates) could diminish the Se risk and toxicity, which enable their effectual application in biomedical/pharmaceutical agents [8,9]. The transformation of Se to its nanostructures was achieved using different protocols, but the biosynthesis using plant derivatives (i.e., phytosynthesis) recently gained more successfulness, because of its elevated efficiency and safety for reducing/stabilizing Se nanoforms [10–15]. The phytosynthesis of nano-Se was also reported to augment their particles' stability, biocompatibility, and bioactivity as antimicrobial, anticancer, and antioxidant agents.

The pomegranate fruits (*Punica granatum* L.) grow in warm climates and their rinds were historically applied as herbaceous remedies for treating and managing numerous disorders, including diarrhea, dysentery, inflammation, cancers, parasitic, and microbial infections [16,17].

The extract of pomegranate rinds (PRE) contains numerous bioactive constituents, e.g., polyphenols, flavonoids, tannins, etc., which have potent antioxidant, antimicrobial, and radical-scavenging mechanisms [18]. Despite its remarkable benefits, PRE is still underutilized [19], but its applications as bio-preservative and antimicrobial agent in food stuffs were recurrently documented [20–23]. Moreover, the high capabilities of PRE for reducing/stabilizing various nanometals (e.g., silver, zinc, and gold) were reported. These potentialities are attributed to PRE's reducing powers and augment the bioactivities of synthesized nanometals with the extract [19,24–26].

Fisheries products (seafoods) and whole fish are vastly perishable and susceptible to microbial contaminations/infections due to their nutritional, biochemical, and compositional structure [27]. Human–fishes interaction/contact and consumption could trigger risks from numerous zoonotic bacterial infections [28]. These bacteria were designated as fish-borne bacterial zoonoses based on phenotypic and epidemiological substantiations [29]. The comprehensively reported zoonotic fish-borne pathogens are *Clostridium* spp. (including *C. botulinum*), *Staphylococcus* spp. (including *S. aureus*), *Vibrio* spp., *Aeromonas* spp., *Mycobacterium* spp., *Streptococcus* spp., *Salmonella* spp. (including *S. typhimurium*), *Sphingomonas* spp. (including *S. paucimobilis*), *Pseudomonas* spp. (including *P. aeruginosa*), and *Edwardsiella* spp. [29–32].

Accordingly, the biosynthesis of Se-nanorods (Se-NRs) using PRE and their characterization were investigated in the present study; the antibacterial actions of biosynthesized nano-Se with PRE were also elucidated toward various fish-borne bacterial pathogens.

2 Materials and methods

2.1 Pomegranate rind extract (PRE) preparation

The pomegranate fruits were organically farmed and harvested at KFS research farm, Kafrelsheikh University, Egypt. Fruits were cleansed accurately with chlorinated water and their rinds were manually peeled, washed with deionized water (DIW), and dried (using hot air at ~43°C for 60 h). The dried rinds were pulverized mechanically, and their powder (~100 g) was soaked in 1,000 mL of 70% of ethanol, agitated with stirrer magnet (at 25 ± 2°C for 72 h, 125×*g*), and filtered to eliminate rind's residues. The PRE was vacuum dried at a temperature of 42°C and pressure of 13.0 kPa, weighed, and re-dissolved in stirred DIW to reach 10% concentration.

2.2 Phytosynthesis of Se-NRs

First, 10 mM solution of sodium selenite (Na_2SeO_3, molar mass: 172.94 g/mol, Sigma-Aldrich, MO) in DIW was prepared. Afterward, equal vol. of PRE (1% concentration) and Na_2SeO_3 solution (10 mL each) were mixed and stirred (540×*g*) with magnetic stirrer for 60 min at 25 ± 2°C. The development of brownish-orange color indicated Se-NRs biosynthesis using PRE. The formed PRE/Se-NRs in reaction solution was precipitated via centrifugation at 12,500×*g* for 35 min (SIGMA 2–16KL centrifuge; Sigma Lab. GmbH, Germany). Then, the portions from the precipitates were washed first by DIW four times and then with ethanol and recentrifuged after each washing to obtain plain Se-NRs [33]. The plain Se-NRs and the PRE/Se-NRs composite were subsequently freeze-dried and characterized.

2.3 Characterization

2.3.1 FTIR spectroscopic analysis

For detecting the distinctive biochemical bonding and interactions in the produced materials as well as their potential

compositions, the PRE and PRE/Se-NRs spectra were spectrophotometrically investigated operating Fourier transform infrared spectroscopy (FTIR) (JASCO FT-IR-360, Tokyo, Japan). The transmission was appraised at 450–4,000/cm wavenumber range.

2.3.2 Se-NRs' optical analysis

For validating the formation of metal NPs, via detecting their surface plasmon resonance associated with free electrons on formed NPs' surfaces, the Se-NRs' spectrum were analyzed by UV-Vis spectrophotometer (model UV-2450, Shimadzu, Japan) at 300–1,000 nm wavelength range.

2.3.3 NRs' size and charge

The appraising of Se-NRs' size (Ps) and zeta potential (ζ) were performed via dynamic light scattering technique, applying zetasizer (Zeta plus, Brookhaven, USA).

2.3.4 NRs' ultrastructure

The Se-NRs ultrastructure, e.g., size and shape, was observed by scanning electron microscope (SEM) (JSM IT100, JEOL, Tokyo, Japan), operating at accelerating voltage of 20 kV.

2.4 Antibacterial assay

The generated agents (PRE, Se-NRs, and PRE/Se-NRs composite) were assessed as antibacterials against fish-borne pathogens including Gram positive ($Gram^+$; *Staphylococcus aureus* [ATCC 25923]) and Gram-negative bacterial strains ($Gram^-$; *Pseudomonas aeruginosa* [ATCC 25006], *Escherichia coli* [ATCC 25922], *Salmonella typhimurium* [ATCC 23852], and *Sphingomonas paucimobilis* [NCTC 11030]). Microorganisms were routinely propagated, maintained, and subcultured aerobically using nutrient broth/agar (NB and NA) (Difco Laboratories, Detroit, MI), at 37°C. Ampicillin (Sigma-Aldrich, MO., CAS no. 69-52-3) was employed as positive antibacterial standard, whereas DIW served as negative control.

2.4.1 Qualitative assay

The "zones of inhibition (ZOI) by disc diffusion assay" was appraised as indicator for bacterial inhibitory action of inspected agents [34]. Concisely, solutions (10% in DIW) were made from each agent and sterile paper discs (Whatman No. 2, 6 mm diameter) were impregnated with solutions to carry 50 µg/disc. Bacteria were spread onto the NA plates and the assay discs were positioned onto the inoculated plates' surface. Then the plates were incubated aerobically at 37°C for 18–24 h until the appearance of growth-free zones around the discs. The mean values of the appeared ZOIs' diameters were appraised from triplicated trials.

2.4.2 Quantitative assay

The minimal inhibitory concentrations (MICs, mg/L), assessment, of each inspected agent toward each pathogen, were implemented thru microdilution technique [22,34], validating results with triphenyl tetrazolium chloride (TTC) staining (Sigma-Aldrich, MO., 5 mg/mL in DIW). Gradual concentrations of PRE, Se-NRs, or PRE/Se-NRs composite (10–100 µg/mL) in NB were prepared in microtiter plates (96 well) and each well was inoculated with ~2×10^6 cells/mL of each individual pathogen. The plates were incubated for 24 h and the free wells from cells' growth (with no obvious turbidity) were treated with 100 µL of TTC solution. 100 µL from the color-free wells (without red formazan formation) were streaked onto the NA plates and the growth-free plates confirmed the agents' inhibitory actions.

2.4.3 Antibacterial visualization via electron microscopy

The SEM photo capturing, of *S. paucimobilis* exposed to PRE/Se-NRs composite, was employed for perceiving structural and morphological alterations/distortions in cells, after exposure to composite for 0, 4, and 8 h, to elucidate its potential action mode. The SEM bacterial imaging applied standardized procedure [35]. Grown bacteria in NB (24 h old) were exposed to 100 µg/mL of composite and incubated at 37°C. Bacterial samples were centrifuged 4,500×*g* for 30 min, washed with 0.9 % NaCl solution, re-centrifuged and then subjected to SEM preparing and imaging.

2.5 Statistical analysis

The mean values ± standard deviation (SD) of triplicated experiments were calculated using SPSS package (SPSS

V-11.5, Chicago, IL, USA),. Results' significances at $p \leq 0.05$ were computed using *t*-test and one-way ANOVA.

3 Results and discussion

3.1 Phytosynthesis and characterization of biosynthesized Se-NRs using PRE

3.1.1 Visual and optical observation

By using PRE, Na_2SeO_3 was bioreduced to Se-NRs, which was visually evidenced by gradual change in solution color from bale yellow to the appearance of deep brownish-orange color after 60 min (1 in Figure 1), signifying the Se-NRs biosynthesis [8]. The UV analysis of PRE-synthesized Se-NRs shows two strong peaks positioned at 464 and 581 nm and one weak peak at 349 nm (2 in Figure 1). These peaks are adjacent to the absorption peaks at 346, 450, and 570 nm for t-Se nanowires found in C12EO10 micelles and at 347, 462, and 586 nm which were reported for Se-NRs spectrum [36].

As formerly reported, the different properties of Se nanomaterials are according to the size and microstructure of the materials and thus could be altered by changing the synthetic conditions [37]. The peaks above 530 nm can be solely ascribed to inter-chain interactions vertical to the c axis within a given t-Se crystal. Therefore, the location of the low-energy peak at high wavelength may provide useful information for the inter-chain interactions in addition to the degree of crystallinity [14,15,33].

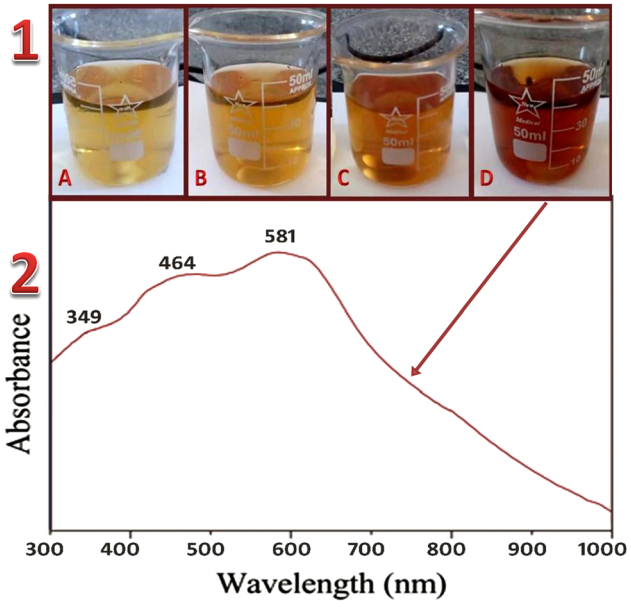

Figure 1: Color indicators of Se-NRs synthesis by pomegranate rind extract showing: (1) visual appearance after incubation for 0 (A), 20 (B), 40 (C), and 60 min (D); and (2) UV-Vis spectrum of biosynthesized Se-NRs.

3.1.2 Size and charge of PRE-synthesized Se-NRs

The Ps analysis of phytosynthesized Se-NRs, mediated by PRE, revealed that their size ranged from 28.41 to 92.61 nm, with mean and median diameters of 62.31 and 64.53 nm, respectively. The mean diameter was the ζ – average hydrodynamic diameter. The resulted green phytosynthesis of Se-NRs is simple, cost effective, and eco-friendly; the resultant NPs have non-toxic and high stability attributes [12]. Additionally, the ζ potential of Se-NRs was computed to be –32 mV, which indicates high stability of NRs in aqueous solution and advocates the PRE stabilization potentiality [38]. ζ potential can provide a definite measurement of specific molecular surface charges, and additionally, it provides indications of the produced electric double layer by the contiguous ions in solution. Characteristically, the NPs with greater ζ values than +30 mV or lesser than –30 mV display higher degrees of stability due to their elevated inter-particle electrostatic repulsion [14,15,33,37].

3.1.3 FTIR analysis

The biochemical bonding and reactions of PRE and PRE/Se-NRs were detectable from their FTIR spectra (Figure 2). The IR pattern of PRE (upper curve in Figure 2) reflected the key attributes of the extract structure. The wide absorption band at 3376.41/cm distinguishes the O–H group in PRE polyphenols, flavonoids, and terpenes, whereas the clear band at 2912.15/cm corresponds to C–H vibrated stretching of alkyl [19,39]. The PRE absorption peaks at 1442.88/cm (aromatic rings) and 1311.21/cm (N–O stretches of nitro compound) were clearly detected in extracted IR spectrum [18,40].

The detectable sharp peaks at 1632.23 and 1741.74/cm are assumingly referring to N–H vibration (in primary amines) and C═O (carbonyls) stretching, respectively [25,41]. The peak at 1042.11/cm, assigning the variable C–O covalent stretching in PRE, was shifted after conjugation with Se-NRs, indicating their combined interactions [24,42].

After conjugation of Se-NRs and their reduction with PRE (lower curve in Figure 2), the O–H wide band shifted

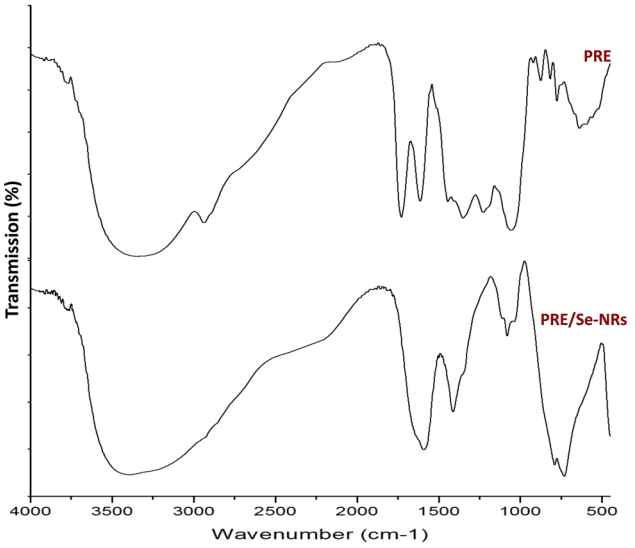

Figure 2: FTIR patterns for the extract of pomegranate rinds (PRE) and phytosynthesized Se-Nanorods with the extract (PRE/Se-NRs).

and the C–H band (at 2912/cm) disappeared, which indicated their roles in Se-NRs reduction/conjugation [19]. Also, the disappearance of C═O stretching band (at 1742/cm), in PRE/Se-NRs spectrum, strongly indicates the involvement of this biochemical bonding in Se-NRs' biosynthesis and the interaction between Se and this bond in PRE [25,41]. The alteration in PRE aromatic rings and N–O designative bands' intensities (after conjugation with Se-NRs) indicated their potential interactions with biosynthesized NPs [19,40]. The strong band, appearing at 723.12/cm in PRE/Se-NRs spectrum, designates the vibrated bending of Se–O, which clearly evidenced the Se-NRs' interaction and stabilization by the PRE [23,26]. The reductions/stabilizations of various Se-NP forms (e.g., nanospheres, nanowires, or nanorods) principally depend on the nature of the stabilizer's capability to interact with Se ions [43,44]. Thus, PRE could be proposed as ideal reducer/stabilizer for biosynthesis of Se-NRs.

3.1.4 SEM imaging

The SEM technique was employed for visualizing the size and shape of the phytosynthesized Se-NRs using PRE (Figure 3). The bioformation of Se-NRs and their morphological dimensions appeared as rod-shape clusters with average rods' diameter of ~64.42 nm and length range from 443.51 to 1236.86 nm, which harmonized the obtained figures from Ps analysis. These Se-NRs' diameter and length are lesser than those obtained in previous study [44], in which the rods' diameter range was 100–200 nm

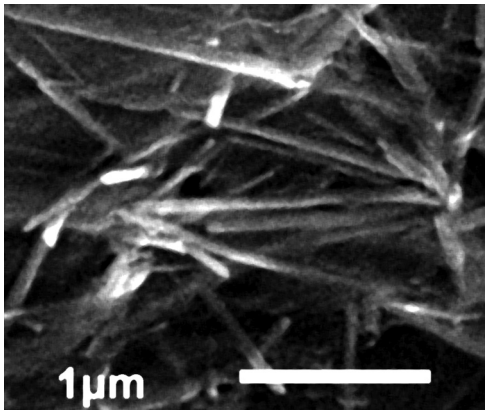

Figure 3: SEM imaging for the structural features of Se-NRs synthesized with pomegranate rind extract.

and length was 1,000–3,000 nm, indicating the high reducing efficiency of PRE to biosynthesize Se-NRs. Furthermore, the complete synthesis of Se-NRs within 6 h of bioreaction with PRE indicates the efficacy of the extract as the bioformation of Se-NRs normally needs long time (up to 48 h) for giving that structure [8].

3.2 Antimicrobial assay

3.2.1 Qualitative and quantitative assays

The assessment of PRE, phytosynthesized Se-NRs, and PRE/Se-NRs composites as antibacterial agents (qualitatively using ZOI and quantitatively using MIC) verified the bacterial inhibitory action of the entire agents (Table 1). Generally, the $Gram^+$ strain (*S. aureus*) had higher resistance than $Gram^-$ species (*P. aeruginosa*, *E. coli*, *S. typhimurium*, and *S. paucimobilis*) toward all examined agents/composite. Oppositely, *S. paucimobilis* showed the highest sensitivity to antibacterial agents, which were proved by the widest ZOIs and least MICs within the challenged strains. The PRE/Se-NRs composites' action were significantly the most forceful, whereas the actions of PRE and Se-NRs were comparable. The PRE/Se-NRs exhibited powerful antibacterial activities, which were insignificantly different from the standard antibiotic (ampicillin), toward the entire challenged strains.

The $Gram^+$ strain (*S. aureus*) was illustrated to have more resistance to biosynthesized Se-NPs than $Gram^-$ species [13,33,45], which harmonizes the current obtained findings for PRE-synthesized Se-NRs.

The $Gram^+$ bacteria are assumed to possess higher resistance to antimicrobial nanometals than $Gram^-$ species due to the presence of $Gram^+$ thick protective

Table 1: Antimicrobial performance of pomegranate rind extract (PRE), biosynthesized selenium nanorods (Se-NRs), and PRE/Se-NRs composites, using zone of inhibition (ZOI; in mm) and minimal inhibitory concentrations (MIC; in mg/L) assays

Antibacterial agent	Antibacterial activity**									
	Staphylococcus aureus		*Pseudomonas aeruginosa*		*Escherichia coli*		*Salmonella typhimurium*		*Sphingomonas paucimobilis*	
	ZOI*	MIC	ZOI	MIC	ZOI	MIC	ZOI	MIC	ZOI	MIC
PRE	13.3 ± 0.7^{a}	72.5	15.9 ± 1.2^{a}	67.5	16.4 ± 1.5^{a}	65.0	14.4 ± 1.0^{a}	70.0	17.7 ± 1.2^{a}	55.0
Se-NRs	15.2 ± 1.1^{b}	60.0	17.4 ± 1.8^{a}	50.0	17.6 ± 1.6^{a}	50.0	15.9 ± 1.4^{a}	55.0	19.6 ± 1.6^{a}	45.0
PRE/Se-NRs	17.1 ± 1.4^{b}	55.0	21.4 ± 2.1^{b}	45.0	20.1 ± 1.7^{b}	47.5	18.4 ± 1.7^{b}	50.0	23.5 ± 2.2^{b}	42.5
Ampicillin	17.7 ± 1.5^{b}	52.5	22.7 ± 2.2^{b}	37.5	29.8 ± 1.4^{b}	40.0	19.1 ± 1.5^{b}	45.0	23.9 ± 1.9^{b}	37.5

*Inhibition zones impart triplicates diameter mean values ± SD, assay discs (diameter 6 mm) carrying 50 µg from PRE, washed Se-NRs, or their blend (PRE/Se-NRs).

**Dissimilar superscript letters within the same column indicate significant difference at $p < 0.05$.

peptidoglycan layer that contains teichoic/lypoteichoic acids. While the Gram^{-} bacteria have specific proteins (porines) that selectively permit molecules' penetration into cells, thus the generated reactive oxygen species (ROS) from Se-NPs can diffuse more easily to interior Gram^{-} cells and destruct/inactivate their vital components [33,46,47].

3.2.2 Antibacterial elucidation via SEM

The consequences of *S. paucimobilis* exposure to PRE/Se-NRs composite on cellular structure, morphology, and deformation are indicated via SEM imaging (Figure 4).

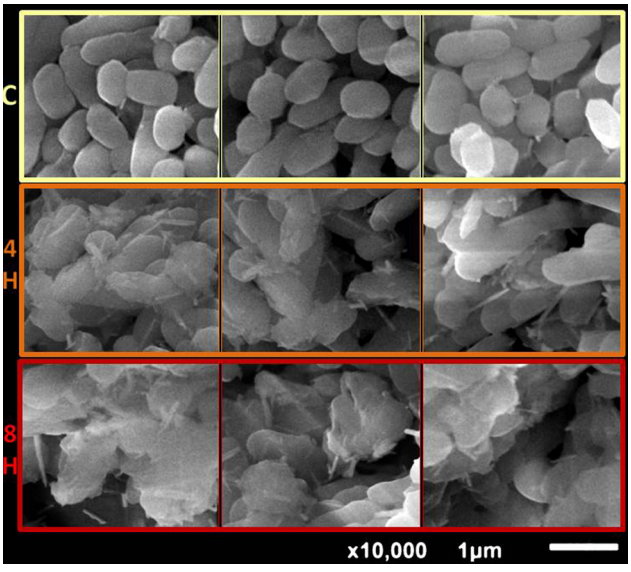

Figure 4: SEM micrographic examples of treated *Sphingomonas paucimobilis* by biosynthesized Se-NRs with pomegranate rind extract.

The choice of bacterial strain (*S. paucimobilis*) was based on its greatest sensitivity to challenging nanocomposites and its novelty as challenged pathogen; thus, it was assumed to offer more useful explanations/evidences for composite action. In the experiment initiation (C in Figure 4), cells had normal, healthy, and contracted appearance with smooth surface and uniformed cell walls. Manifested morphological distortions in the bacterial cells were noticed after the 4th h of exposure to PRE/Se-NRs composite. Bacterial walls were expanded, became puffy, and lots of Se-NRs were attached to the outer cell membranes (4H in Figure 4). With PRE/Se-NRs exposure prolongation to 8 h, cells' deformation, distortion, and lyses became very noticeable (8H in Figure 4). The challenged cells were largely exploded/lysed at this stage. The damaged cell wall residues and interior cellular components were mostly intermingled with Se-NRs. The PRE/Se-NRs composite bactericidal actions are assumed to involve synergistic mechanisms from PRE and Se-NRs [48,49].

The PRE was verified for possessing strong microbicidal and sanitizing actions toward numerous pathogenic bacteria, yeast, and fungi, either as distinct extract or mixed with further bioactive molecules [12,20,22,49,50]. The bioactive phytochemical contents in PRE from alkaloids, tannins, flavonoids, and phenolics (e.g., punicalagin, gallotannins, catechins, kaempferol, ellagic acid, castalagin, quercetin, granatin, and gallocatechin) are the key components responsible for its antimicrobial action [16,18,20,21].

The ROS generation and elevated intracellular ROS levels were reported after cells' treatment with biosynthesized Se-NPs [51]. These high ROS levels are frequently associated with mitochondrial dysfunction and DNA damage, leading to cellular death [8]. The PRE-mediated nanometals could have influential antibacterial mechanisms, involving the anchoring/penetration through cell walls and restraining

cellular signals via diverse peptides' dephosphorylation [19,24]. Despite their forceful antibacterial actions, biosynthesized Se-NRs were recommended to possess fascinating attributes for drug delivery because of their diminished side-effects, elevated biocompatibility, and low cytotoxicity [52]. The antibacterial capacities of PRE-mediated metal NPs were reported to depend on the PRE antibacterial action added to NPs' potentialities [26]. Metal NPs with miniature Ps can interact with cellular membranes (as evidently shown in Figure 4), pass into interior cells, and prohibit DNA and protein functions, thereby triggering cells' apoptosis/death, because bacteria cannot habitually replicate. The metallic NPs' (including Se-NPs) antibacterial actions are principally based on generated ROS by NPs, their electrochemical binding to microorganisms' cells, cellular ATP and biomolecule depletion, and cations release [1,7,13]. Additionally, the Se-NPs' bactericidal action was assumed to be associated with osmotic imbalance after interaction among bacterial cells and Se-NPs. This leads to cellular biochemical bonds' interruption in membrane structure and deformation of cell-walls' permeability and functionality [6,15]. The Se-NPs were additionally suggested to interact with thiol and sulfhydryl groups in cellular membrane proteins (e.g., porines), denaturing them, and subsequently causing membranes' deformation and distortion [33].

4 Conclusion

In the presented investigation, PRE was extracted from *P. granatum* rinds and effectively employed for phytosynthesis of Se-NRs. The synthesized NRs were negatively charged and had mean diameter of 62.31 nm. The antibacterial actions of PRE, plain Se-NRs, and PRE/Se-NRs composite were proved toward various fish-borne bacterial pathogens, i.e., *S. aureus*, *P. aeruginosa*, *E. coli*, *S. typhimurium*, and *S. paucimobilis*, which advocate their applicability for decontaminating fish farms and products.

Acknowledgement: The authors are greatly thankful for the mercy help and guidance from ALLAH. The appreciation is indebted for The Central Lap for Aquatic Health and Safety – Kafrelsheikh University (CLAHS-KFS), for providing the required facilities to conduct the study.

Funding information: Authors state no funding involved.

Author contributions: Hend Gad: conceptualization, methodology, investigation, data curation, formal analysis, writing – original draft; Ahmed Tayel: conceptualization, methodology, formal analysis, writing – original draft, writing – review and editing; Mohammed Al-Saggaf: resources, visualization, formal analysis; Shaaban Moussa: resources, project administration, visualization; Amany Diab: conceptualization, supervision, investigation, validation, writing – review and editing.

Conflict of interest: Authors state no conflict of interest.

Data availability statement: The data presented in this study are available on reasonable request from the corresponding author.

References

[1] Slavin YN, Asnis J, Häfeli UO, Bach H. Metal nanoparticles: understanding the mechanisms behind antibacterial activity. J Nanobiotechnol. 2014;15:65. doi: 10.1186/s12951-017-0308-z.
[2] El Shafey AM. Green synthesis of metal and metal oxide nanoparticles from plant leaf extracts and their applications: a review. Green Process Synth. 2020;9(1):304–39. doi: 10.1515/gps-2020-0031.
[3] Reverberi A, Vocciante M, Lunghi E, Pietrelli L, Fabiano B. New trends in the synthesis of nanoparticles by green methods. Chem Eng Trans. 2017;61:667–72. doi: 10.3303/CET1761109.
[4] Khalaj M, Kamali M, Costa MEV, Capela I. Green synthesis of nanomaterials – a scientometric assessment. J Clean Prod. 2020;267:122036. doi: 10.1016/j,jclepro.2020.122036.
[5] Zamani A, Marjani AP, Mousav Z. Agricultural waste biomass-assisted nanostructures: synthesis and application. Green Process Synth. 2019;8(1):421–9. doi: 10.1515/gps-2019-0010.
[6] Mezes M, Balogh K. Prooxidant mechanisms of selenium toxicity – a review. Acta Biol Szeged. 2009;53:15–8.
[7] Zhao G, Wu X, Chen P, Zhang L, Yang CS, Zhang J. Selenium nanoparticles are more efficient than sodium selenite in producing reactive oxygen species and hyper-accumulation of selenium nanoparticles in cancer cells generates potent therapeutic effects. Free Radic Biol Med. 2018;126:55–66. doi: 10.1016/j.freeradbiomed.
[8] Ahmad MS, Yasser MM, Sholkamy EN, Ali AM, Mehanni MM. Anticancer activity of biostabilized selenium nanorods synthesized by streptomyces bikiniensis strain Ess_amA-1. Int J Nanomed. 2015;2015(10):3389. doi: 10.2147/iJN.S82707.
[9] Kumar A, Prasad KS. Role of nano-selenium in health and environment. J Biotechnol. 2021;325:152–63. doi: 10.1016/j.jbiotec.2020.11.004.
[10] Alsaggaf MS, Moussa SH, Tayel AA. Application of fungal chitosan incorporated with pomegranate peel extract as edible coating for microbiological, chemical and sensorial quality enhancement of Nile tilapia fillets. Int J Bio Macromol. 2017;99:499–505. doi: 10.1016/j.ijbiomac.2017.03.017.

[11] Fardsadegh B, Jafarizadeh-Malmiri H. *Aloe vera* leaf extract mediated green synthesis of selenium nanoparticles and assessment of their in vitro antimicrobial activity against spoilage fungi and pathogenic bacteria strains. Green Process Synth. 2019;8(1):399–407. doi: 10.1515/gps-2019-0007.
[12] Fardsadegh B, Vaghari H, Mohammad-Jafari R, Najian Y, Jafarizadeh-Malmiri H. Biosynthesis, characterization and antimicrobial activities assessment of fabricated selenium nanoparticles using *Pelargonium zonale* leaf extract. Green Process Synth. 2019;8(1):191–8. doi: 10.1515/gps-2018-0060.
[13] Alghuthaymi MA, Diab AM, Elzahy AF, Mazrou KE, Tayel AA, Moussa SH. Green biosynthesized selenium nanoparticles by cinnamon extract and their antimicrobial activity and application as edible coatings with nano-chitosan. J Food Qual. 2021;2021:6670709. doi: 10.1155/2021/6670709.
[14] ElSaied BE, Diab AM, Tayel AA, Alghuthaymi MA, Moussa SH. Potent antibacterial action of phycosynthesized selenium nanoparticles using *Spirulina platensis* extract. Green Process Synth. 2021;10(1):49–60. doi: 10.1515/gps-2021-0005.
[15] Yilmaz MT, İspirli H, Taylan O, Dertli EA. green nano-biosynthesis of selenium nanoparticles with Tarragon extract: Structural, thermal, and antimicrobial characterization. LWT. 2021;141:110969. doi: 10.1016/j.lwt.2021.110969.
[16] Jayaprakasha GK, Negi PS, Jena BS. Antimicrobial activities of pomegranate. In: Seeram NP, Schulman RN, Heber D, editors. Pomegranates: ancient roots to modern medicine. Boca Raton, FL, USA: CRC Press; 2006. p. 167–83.
[17] Zarfeshany A, Asgary S, Javanmard SH. Potent health effects of pomegranate. Adv Biomed Res. 2014;3:100. doi: 10.4103/2277-9175.129371.
[18] Ben-Ali S, Akermi A, Mabrouk M, Ouederni A. Optimization of extraction process and chemical characterization of pomegranate peel extract. Chem Papers. 2018;72(8):2087–100. doi: 10.1007/s11696-018-0427-5.
[19] Manna K, Mishra S, Saha M, Mahapatra S, Saha C, Yenge G, et al. Amelioration of diabetic nephropathy using pomegranate peel extract-stabilized gold nanoparticles: assessment of NF-κB and Nrf2 signaling system. Int J Nanomed. 2019;14:1753. doi: 10.2147/Ljn.S176013.
[20] Tayel AA, El-Baz AF, Salem MF, El-Hadary MH. Potential applications of pomegranate peel extract for the control of citrus green mould. J Plant Dis Prot. 2009;116(6):252–6. doi: 10.1007/BF03356318.
[21] Tayel AA, El-Tras WF. Anticandidal activity of pomegranate peel extract aerosol as an applicable sanitizing method. Mycoses. 2010;53(2):117–22. doi: 10.1111/j.1439-0507.2008.01681.x.
[22] Tayel AA, El-Tras WF. Plant extracts as potent biopreservatives for *Salmonella typhimurium* control and quality enhancement in ground beef. J Food Safe. 2012;32(1):115–21. doi: 10.1111/j1745-4565.2011.00357.x.
[23] Surendhiran D, Li C, Cui H, Lin L. Fabrication of high stability active nanofibers encapsulated with pomegranate peel extract using chitosan/PEO for meat preservation. Food Packag Shelf Life. 2020;23:100439. doi: 10.1016/j.fpsl.2019.100439.
[24] Shanmugavadivu M, Kuppusamy S, Ranjithkumar R. Synthesis of pomegranate peel extract mediated silver nanoparticles and its antibacterial activity. Am J Adv Drug Deliv. 2014;2(2):174–82.
[25] Joshi SJ, Al-Mamari S, Al-Azkawi A. Green synthesis of silver nanoparticles using pomegranate peel extracts and its application in photocatalytic degradation of methylene blue. Jundishapur J Nat Pharm Prod. 2018;13(3):e67846. doi: 10.5812/jjnpp.67846.
[26] Sukri SNAM, Shameli K, Wong MMT, Teow SY, Chew J, Ismail NA. Cytotoxicity and antibacterial activities of plant-mediated synthesized zinc oxide (ZnO) nanoparticles using *Punica granatum* (pomegranate) fruit peels extract. J Mol Struct. 2019;1189:57–65. doi: 10.1016/J.MOLSTRUC.2019.04.026.
[27] Ali A, Parisi A, Conversano MC, Iannacci A, D'Emilio F, Mercurio V, et al. Food-borne bacteria associated with seafoods: a brief review. J Food Qual Hazards Control. 2020;7:4–10. doi: 10.18502/jfqhc.7.1.2446.
[28] Pękala-Safińska A. Contemporary threats of bacterial infections in freshwater fish. J Vet Res. 2018;62(3):261. doi: 10.2478/jvetres-2018-0037.
[29] Gauthier DT. Bacterial zoonoses of fishes: a review and appraisal of evidence for linkages between fish and human infections. Vet J. 2015;203(1):27–35. doi: 10.1016/j.tvjl.2014.10.028.
[30] El Bayomi RM, Darwish WS, El-Moaty AMA, Gad TM. Prevalence, antibiogram, molecular characterization and reduction trial of *Salmonella typhimurium* isolated from different fish species. Jpn J Vet Res. 2016;64(2):S181–6.
[31] Boss R, Overesch G, Baumgartner A. Antimicrobial resistance of *Escherichia coli*, Enterococci, *Pseudomonas aeruginosa*, and *Staphylococcus aureus* from raw fish and seafood imported into Switzerland. J Food Prot. 2016;79(7):1240–6. doi: 10.4315/0362-028X.
[32] Hoque F, Abraham TJ, Jaisankar P. Isolation and partial characterisation of secondary metabolites from fish-borne bacterium, *Pseudomonas aeruginosa*. Indian J Fish. 2019;66(1):81–91. doi: 10.21077/ijf.2019.66.1.79940-11.
[33] Menon S, Agarwal H, Rajeshkumar S, Rosy PJ, Shanmugam VK. Investigating the antimicrobial activities of the biosynthesized selenium nanoparticles and its statistical analysis. Bionanoscience. 2020;10:122–35. doi: 10.1007/s12668-019-00710-3.
[34] Tayel AA, El-Tras WF, Moussa S, El-Baz AF, Mahrous H, Salem MF, et al. Antibacterial action of zinc oxide nanoparticles against foodborne pathogens. J Food Safe. 2011;31(2):211–8. doi: 10.1111/j.1745-4565.2010.00287.x.
[35] Marrie T, Costerton JW. Scanning and transmission electron microscopy of in situ bacterial colonization of intravenous and intraarterial catheters. J Clin Microbiol. 1984;19(5):687–93. doi: 10.1128/jcm.19.5.687-693.1984.
[36] Ma Y, Qi L, Shen W, Ma J. Selective synthesis of single-crystalline selenium nanobelts and nanowires in micellar solutions of nonionic surfactants. Langmuir. 2005;21(14):6161–4. doi: 10.1021/la050801l.
[37] Chen H, Yoo JB, Liu Y, Zhao G. Green synthesis and characterization of Se nanoparticles and nanorods. Electron Mater Lett. 2011;7(4):333–6. doi: 10.1007/s13391-011-0420-4.
[38] Presentato A, Piacenza E, Anikovskiy M, Cappelletti M, Zannoni D, Turner RJ. Biosynthesis of selenium-nanoparticles and-nanorods as a product of selenite bioconversion by the aerobic bacterium Rhodococcus aetherivorans BCP1. N Biotechnol. 2018;41:1–8. doi: 10.1016/j.nbt.2017.11.002.
[39] Oliveira RN, Mancini MC, Oliveira FCSD, Passos TM, Quilty B, Thiré RMDSM, et al. FTIR analysis and quantification of

phenols and flavonoids of five commercially available plants extracts used in wound healing. Matéria (Rio de Janeiro). 2016;21(3):767–79. doi: 10.1590/S1517-707620160003.0072.
[40] Ganeshkumar M, Sathishkumar M, Ponrasu T, Dinesh MG, Suguna L. Spontaneous ultra fast synthesis of gold nanoparticles using Punica granatum for cancer targeted drug delivery. Colloids Sur B. 2013;106:208–16. doi: 10.1016/j.colsurfb.2013.01.035.
[41] Edison TJI, Sethuraman MG. Biogenic robust synthesis of silver nanoparticles using Punica granatum peel and its application as a green catalyst for the reduction of an anthropogenic pollutant 4-nitrophenol. Mol Biomol Spectrosc. 2013;104:262–4. doi: 10.1016/j.saa.2012.11.084.
[42] Kannan S, Mohanraj K, Prabhu K, Barathan S, Sivakumar G. Synthesis of selenium nanorods with assistance of biomolecule. Bull Mater Sci. 2014;37(7):1631–5. doi: 10.1007/s12034-014-0712-z.
[43] Refat MS, Elsabawy KM. Infrared spectra, Raman laser, XRD, DSC/TGA and SEM investigations on the preparations of selenium metal (Sb_2O_3, Ga_2O_3, SnO and HgO) oxides and lead carbonate with pure grade using acetamide precursors. Bull Mater Sci. 2011;34(4):873. doi: 10.1007/s12034-011-0208-z.
[44] Wang Q, Mejia Jaramillo A, Pavon JJ, Webster TJ. Red selenium nanoparticles and gray selenium nanorods as antibacterial coatings for PEEK medical devices. J Biomed Mater Res B Appl Biomater. 2016;104(7):1352–8. doi: 10.1002/jbm.b.33479.
[45] AlSaggaf MS, Tayel AA, Ghobashy MO, Alotaibi MA, Alghuthaymi MA, Moussa SH. Phytosynthesis of selenium nanoparticles using the costus extract for bactericidal application against foodborne pathogens. Green Process Synth. 2020;9(1):477–87. doi: 10.1515/gps-2020-0038.
[46] Breijyeh Z, Jubeh B, Karaman R. Resistance of Gram-negative bacteria to current antibacterial agents and approaches to resolve it. Molecules. 2020;25(6):1340. doi: 10.3390/molecules25061340.
[47] Grigoreva A, Saranina I, Tikunova N, Safonov A, Timoshenko N, Rebrov A, et al. Fine mechanisms of the interaction of silver nanoparticles with the cells of Salmonella typhimurium and Staphylococcus aureus. Biometals. 2013;26(3):479–88. doi: 10.1007/s10534-013-9633-3.
[48] Osaili TM, Albiss B, Al–Nabulsi A, Alromi AA, Olaimat RF, Al-Holy A M, et al. Effects of metal oxide nanoparticles with plant extract on viability of foodborne pathogens. J Food Safe. 2019;39(5):e12681. doi: 10.1111/jsf.12681.
[49] Alotaibi MA, Tayel AA, Zidan NS, El Rabey HA. Bioactive coatings from nano-biopolymers/plant extract composites for complete protection from mycotoxigenic fungi in dates. J Sci Food Agric. 2021;99(9):4338–43. doi: 10.1002/jsfa.9667.
[50] Tayel AA, Moussa SH, Salem MF, Mazrou KE, El-Tras WF. Control of citrus molds using bioactive coatings incorporated with fungal chitosan/plant extracts composite. J Sci Food Agric. 2016;96(4):1306–12. doi: 10.1002/jsfa.7223.
[51] Li H, Liu D, Li S, Xue C. Synthesis and cytotoxicity of selenium nanoparticles stabilized by α-D-glucan from *Castanea mollissima* Blume. Int J Biol Macromol. 2019;129:818–26. doi: 10.1016/j.ijbiomac.2019.02.085.
[52] Velayati M, Hassani H, Sabouri Z, Mostafapour A, Darroudi M. Biosynthesis of Se-Nanorods using Gum Arabic (GA) and investigation of their photocatalytic and cytotoxicity effects. Inorg Chem Commun. 2021;128:108589. doi: 10.1016/j.inoche.